Transfer-Free Synthesis of Doped and Patterned Graphene Films

Qi-Qi Zhuo, Qi Wang, Yi-Ping Zhang, Duo Zhang, Qin-Liang Li, Chun-Hong Gao, Yan-Qiu Sun, Lei Ding, Qi-Jun Sun, Sui-Dong Wang, Jun Zhong, Xu-Hui Sun,* and Shuit-Tong Lee

Institute of Functional Nano & Soft Materials (FUNSOM) and Jiangsu Key Laboratory for Carbon-Based Materials and Devices, Soochow University, 199 Renai Road, Suzhou, Jiangsu 215123, China

ABSTRACT

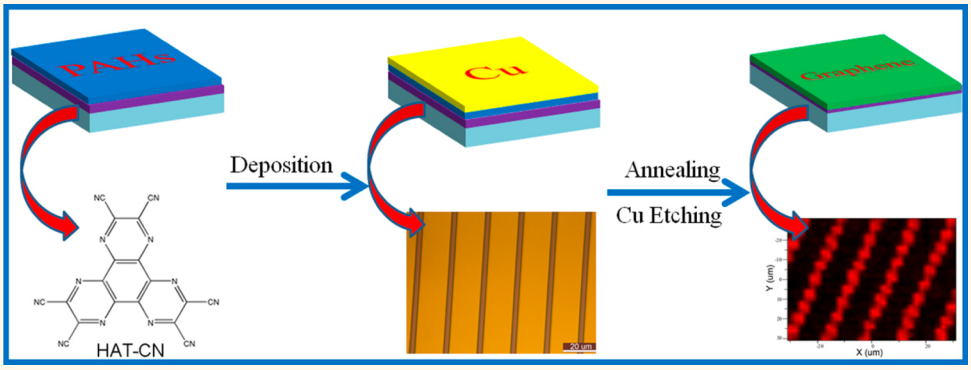

High-quality and wafer-scale graphene on insulating gate dielectrics is a prerequisite for graphene electronic applications. For such applications, graphene is typically synthesized and then transferred to a desirable substrate for subsequent device processing. Direct production of graphene on substrates without transfer is highly desirable for simplified device processing. However, graphene synthesis directly on substrates suitable for device applications, though highly demanded, remains unattainable and challenging. Here, we report a simple, transfer-free method capable of synthesizing graphene directly on dielectric substrates at temperatures as low as 600 °C using polycyclic aromatic hydrocarbons as the carbon source. Significantly, N-doping and patterning of graphene can be readily and concurrently achieved by this growth method. Remarkably, the graphene films directly grown on glass attained a small sheet resistance of 550 Ω/sq and a high transmittance of 91.2%. Organic light-emitting diodes (OLEDs) fabricated on N-doped graphene on glass achieved a current density of 4.0 mA/cm^2 at 8 V compared to 2.6 mA/cm^2 for OLEDs similarly fabricated on indium tin oxide (ITO)-coated glass, demonstrating that the graphene thus prepared may have potential to serve as a transparent electrode to replace ITO.

KEYWORDS: graphene · transfer-free · doped · patterned · polycyclic aromatic hydrocarbons

Graphene has attracted intense interest due to its outstanding properties such as high carrier mobility, optical transparency, mechanical flexibility, low density, and chemical stability.[1,2] Since the successful isolation of graphene *via* mechanical exfoliation of graphite,[3,4] various methods of graphene synthesis have been developed, including chemical vapor deposition (CVD),[5−7] chemical reduction of graphene oxides,[8−10] and organic synthesis from micromolecules.[11,12] Among the methods, graphene synthesis by CVD on metal catalyst films has unique advantages for large-area and uniform graphene formation for electronic applications. However, in all methods, it is necessary to physically transfer the grown graphene onto desired substrates for subsequent device processing. During the transfer process, great care must be taken to avoid introducing defects into the graphene sheet. Hence, intense efforts have focused on developing alternative synthetic methods that can avoid transfer. Ismach *et al.*[13] reported that graphene grown by CVD on a Cu layer can be directly deposited onto a quartz substrate by evaporating the Cu layer with a prolonged high-temperature treatment. Byun *et al.*[14] thermally converted organic polymers coated on an insulator substrate to graphene by a Ni capping layer at 1000 °C. Afterward, the Ni layer was etched away, leaving graphene on the insulator substrate.

* Address correspondence to xhsun@suda.edu.cn.

Received for review October 16, 2014 and accepted December 28, 2014.

Published online December 29, 2014
10.1021/nn505913v

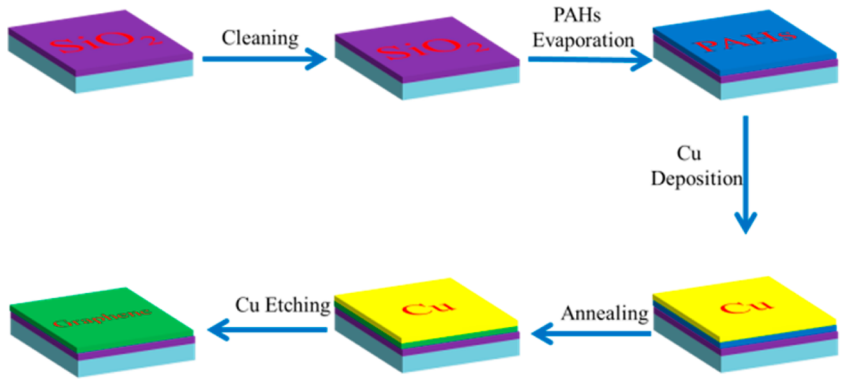

Figure 1. Schematic of the direct synthesis of graphene on SiO_2 without transfer.

However, it is difficult to obtain a uniform graphene sheet due to carbon precipitation from the Ni film during the cooling process.[15] Besides, the high temperature needed for growth further limited its usage. In addition, the direct growth of graphene on insulating substrates such as SiO_2,[16−20] Al_2O_3,[21,22] BN,[23,24] Si_3N_4,[25] quartz,[26−28] and $SrTiO_3$[29] by catalyst-free CVD has also been demonstrated. The syntheses should require high temperature[21,22,30] or long thermal annealing times.[25] Moreover, it is difficult to obtain high-quality and large-size films. A method for direct CVD growth of only few-layer graphene on nonconducting materials remains much needed for electronic and optical applications.

Pristine monolayer graphene exhibits a zero band gap, which limits graphene's electronic and optical applications. Progress has been made in modifying the band gap of graphene, including using special substrates or defining nanoscale graphene ribbons. Another feasible approach to opening the band gap is to replace the carbon atoms in the graphene matrix with heteroatoms such as nitrogen or boron dopants.[16,17,31−33] A doping process to obtain uniformly doped graphene still remains a challenge.[32,34]

Here, we introduce a facile method to synthesize uniform and large-area graphene directly on glass or SiO_2 using a Cu top layer as catalyst and polycyclic aromatic hydrocarbons (PAHs) as the carbon source. PAHs can be simply patterned on different substrates through thermal evaporation or spin-coating through a desirable mask. Moreover, highly nitrogen-doped graphene can be easily obtained at a relatively low temperature by using PAHs containing N atoms.

RESULTS AND DISCUSSION

The present scheme of a direct growth process of graphene on insulating substrates (glass or SiO_2) is shown in Figure 1. First, the 300 nm thick SiO_2/Si wafer is cleaned by ethanol, acetone, and deionized water. Then, PAHs and the Cu layer are deposited on the cleaned wafer as the carbon source and catalyst, respectively. After thermal annealing, graphene is formed between the Cu layer and the insulating SiO_2 substrate. Lastly, the Cu layer is etched off by Marble's reagent ($CuSO_4$/HCl/H_2O = 10 g/50 mL/50 mL), and graphene is obtained directly on the SiO_2 substrate without any transfer process needed.

CVD synthesis of graphene can be divided into several steps:[35−37] adsorption, nucleation, island growth, and island coalescence to form a continuous graphene sheet. The nature of the carbon source is considered to be an important factor for graphene growth. Byun *et al.*[14] used precursors composed of aliphatic C−C single bonds as carbon sources and suggested that the planar zigzag configuration may facilitate cyclization of C−C bonds due to the lower bond dissociation energies of C−C single bonds (284−368 kJ/mol) compared to those of C═C (615 kJ/mol), C≡C (812 kJ/mol), and aromatic/heterocyclic C−C (410 kJ/mol) in the precursors. Wan *et al.*[35] used PAHs as carbon sources and achieved synthesis of graphene at relatively low temperature (550 °C for coronene, 800 °C for pentacene). They think that the C−C bonds in PAHs are unlikely to shatter on the Cu substrate. The graphene growth mechanism from PAHs mainly involves a surface-mediated nucleation process of dehydrogenated PAHs rather than segregation or a precipitation process of small carbon species from precursor decomposition. Using aromatic hydrocarbons as the carbon source can greatly decrease the temperature of graphene growth. For example, using pyridine as both carbon and nitrogen source, Xue *et al.*[32] succeeded in synthesizing N-doped graphene even at a temperature as low as 300 °C.

Here, we choose three different PAHs as the sources to synthesize graphene. Figure 2 shows the atomic force microscopy (AFM) image and Raman spectra of the as-synthesized graphene. Graphene was obtained from all three kinds of PAHs but with different qualities. The graphene from HAT-CN shows a lower D peak than those from ADN and NPB, indicating lower defect level and better single crystallinity of the former graphene. The graphene can even be obtained at 600 °C from HAT-CN (Figure 3c). Because HAT-CN is a planar PAH while both ADN and NPB are nonplanar PAHs, the molecular configuration of PAHs may be a key factor in

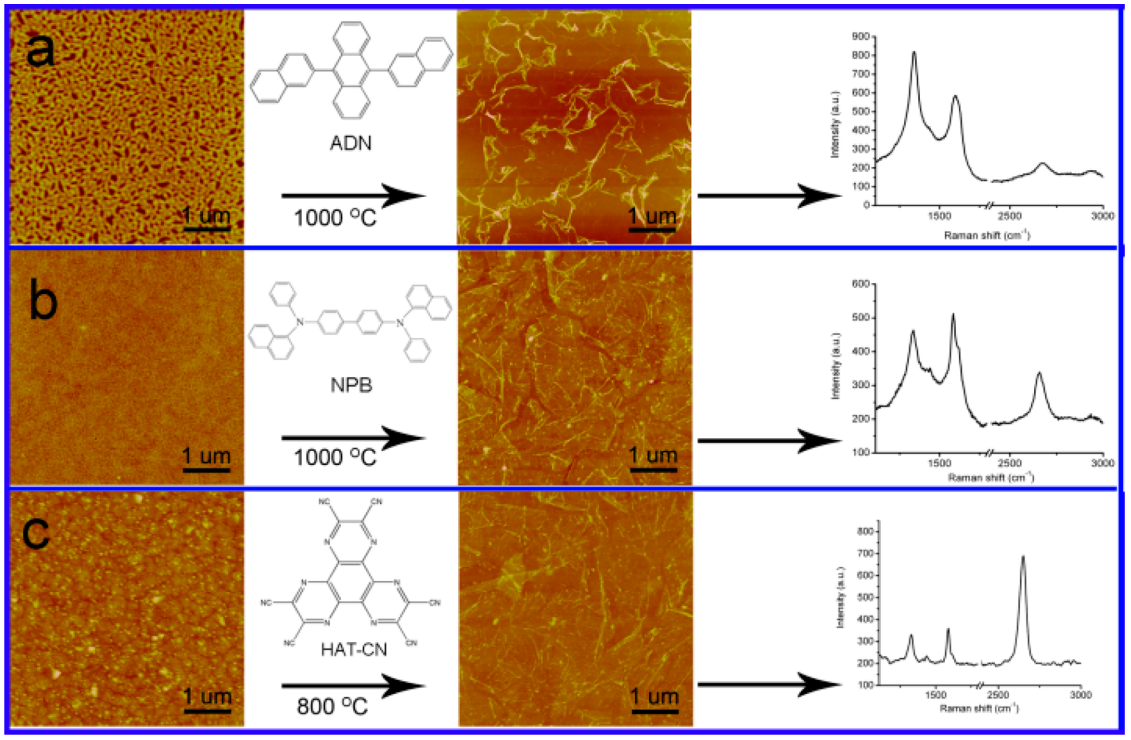

Figure 2. AFM image and Raman spectra of graphene growth under a Cu layer with different PAHs: (a) ADN, (b) NPB, and (c) HAT-CN; their molecular structures are shown in the inset.

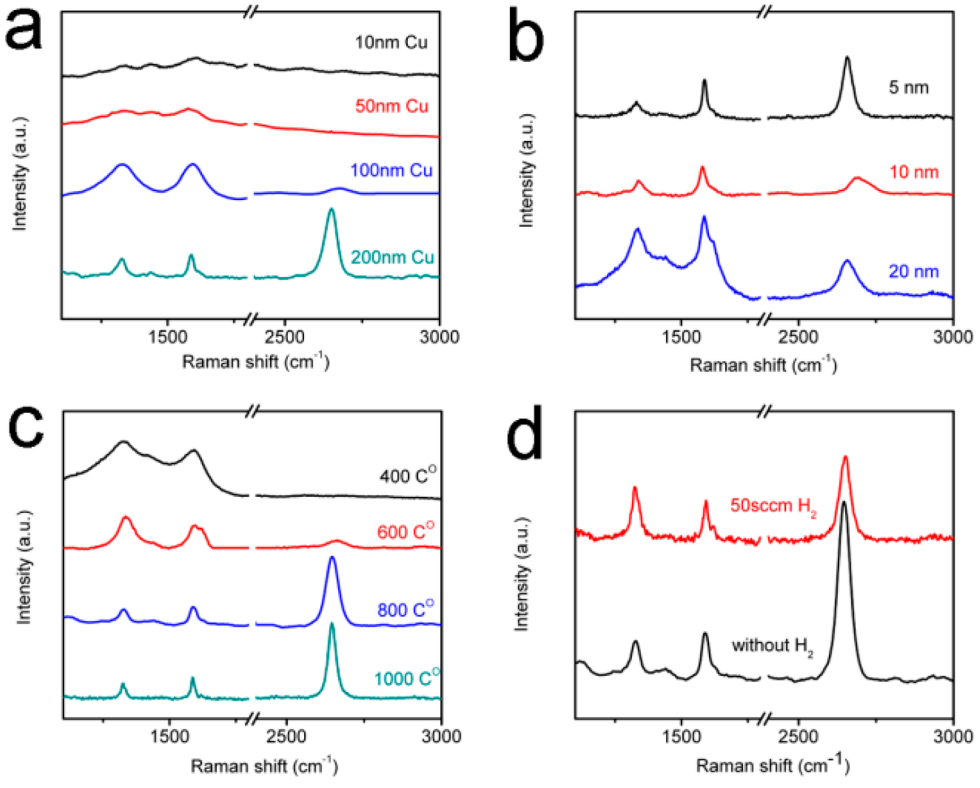

Figure 3. (a) Raman spectra of graphene synthesized by HAT-CN with different Cu thickness. (b) Raman spectra of graphene synthesized with HAT-CN of different thickness. (c) Raman spectra of graphene synthesized at different temperature. (d) Raman spectra of graphene with different content of H_2.

graphene growth. Recently, Wan *et al.*[35] also reported a similar result using coronene, pentacene, and rubrene as the carbon source to grow graphene on a Cu catalyst.

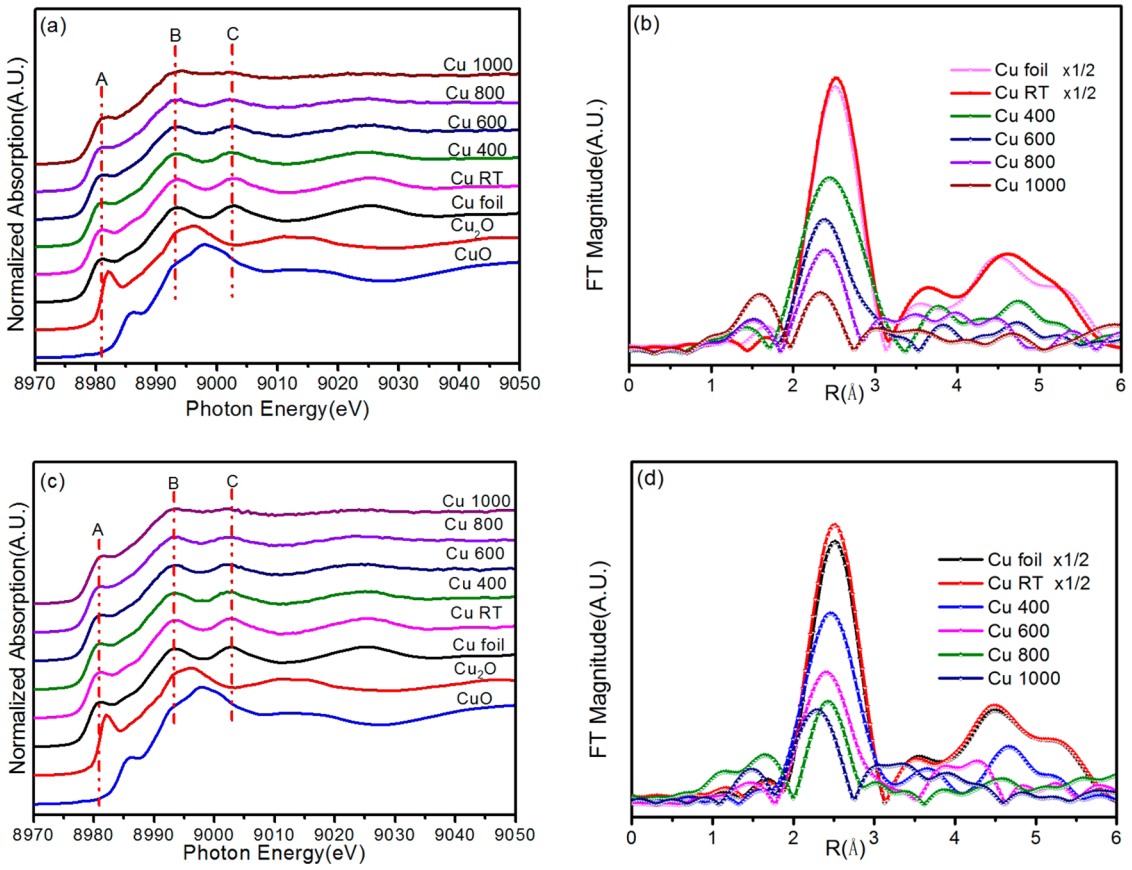

Figure 4. ***In situ*** **XAFS of Cu/HAT-CN (a) and its corresponding Fourier transform magnitudes (b) at different annealing temperature, and** ***in situ*** **XAFS of the Cu layer only (c) and its corresponding Fourier transform magnitudes (d) at the same measurement conditions for comparison.**

The thickness of Cu and PAH layers is found to be very critical to the quality of graphene films grown by the present method. The thickness of Cu and PAHs was optimized to obtain high-quality graphene. The Raman spectra shown in Figure 3a reveal that the optimum thickness of the Cu layer is greater than 100 nm. When thinner Cu (less than 50 nm) was used, the Cu layer would easily agglomerate and partially evaporate from the substrate during the thermal annealing process. Although the thicker Cu layer (more than 200 nm) does not affect the quality of graphene, it will not be economic to use a thicker Cu layer. The optimum Cu layer of 100−200 nm in thickness has been used in the growth process. The thickness effect of PAHs on the quality of graphene was also investigated. For example, 5−10 nm thick HAT-CN provides better-quality graphene (see Figure 3b). It shows that thicker PAHs result in more amorphous carbon formed between the Cu layer and the SiO_2 substrate due to the extremely low solubility of C in Cu. The result supports that the growth mechanism of graphene from PAHs is through the surface-mediated nucleation process.

The growth temperature is another important factor affecting the quality of graphene. In general, the growth temperature in a conventional CVD method using gas precursors to synthesize good-quality graphene generally requires 1000−1050 °C.[6,13,38] Remarkably, the present growth method using PAHs as the carbon source can greatly reduce the growth temperature. Figure 3c shows the Raman spectra of graphene synthesized using HAT-CN at different growth temperatures. Significantly, graphene was formed even at 600 °C. Since hydrogen atoms can etch both sp^2-bonded and amorphous carbon atoms, the amount of hydrogen is also a critical factor affecting the quality of the synthesized graphene.[35,39] Figure 3d shows that the complete absence of hydrogen during the influx of PAHs has a pivotal effect on the quality of the obtained graphene.

To clarify the mechanism of graphene growth with PAHs, we used *in situ* X-ray absorption fine structure (XAFS) spectroscopy to follow the chemical state and local structure of the copper layer during the growth process. The XAFS results in Figure 4 show that no obvious change of the Cu/HAT-CN sample relative to the Cu reference can be found at different temperatures. Also, no Cu−C alloy or Cu compound is formed during the process. It directly demonstrates that the growth of graphene in the present work only occurs on the Cu surface following the surface-mediated nucleation mechanism.[20]

Graphene patterning is essential for electronic and optoelectronic applications. A major advantage of the

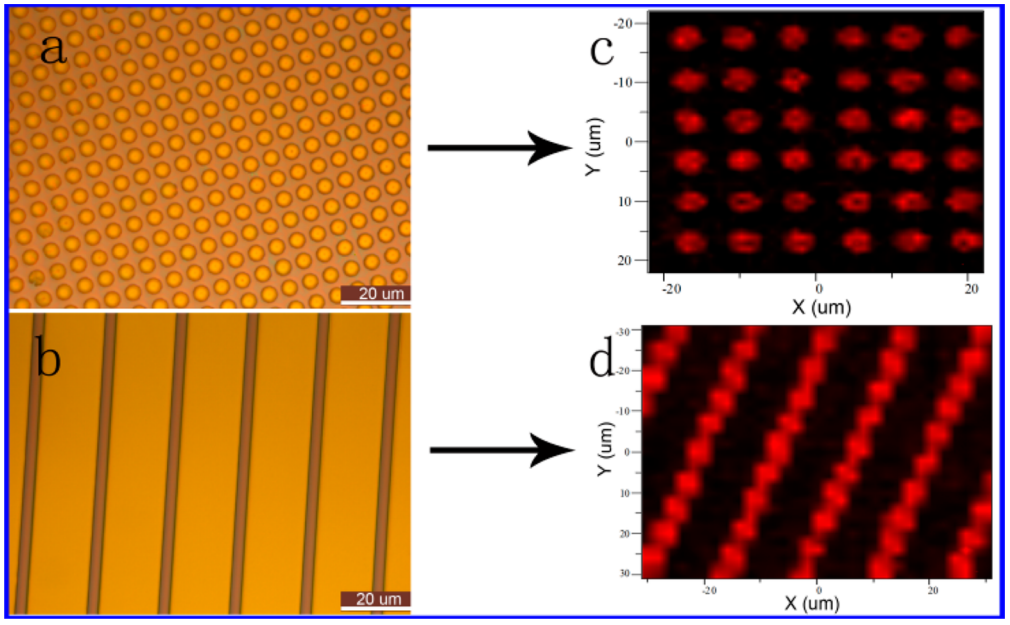

Figure 5. Typical microscope image of PAHs/Cu (a,b) and micro-Raman mapping (c,d) for the 2D graphene peak (~2650 cm^{-1}) with different patterns: (a,c) dots; (b,d) lines.

present growth method is the extreme ease in patterning graphene, which can be simply obtained on the substrate by directly patterning either the PAH precursor layer or the Cu catalyst layer, thus avoiding the need for additional transferring and patterning as required in previous methods.[40] Desired patterns of the PAH layer or Cu layer can be easily generated by shadow mask during the evaporation or photolithography process after the deposition. After being annealed and etched by the residual Cu by Marble's reagent, differently patterned graphene on the substrate can be obtained. Figure 5a−c shows the optical images of PAH/Cu (5 nm/200 nm) with different patterns, while Figure 5d−f shows the corresponding micro-Raman mapping images of the 2D graphene peak (~2650 cm^{-1}) of the subsequent graphene. In addition, the Raman mapping images of I_G/I_D and the I_{2D}/I_G graphene are shown in Supporting Information Figure S1, which further verify the uniformity of the quality (I_G/I_D) and the number of layers (I_{2D}/I_G), respectively.

Another advantage of the present method is that doping of graphene can be simply achieved by using the PAH precursor containing a dopant element. For example, N-doping can be achieved by using HAT-CN as the precursor. Raman spectra of N-doped graphene are shown in Figure S2 (Supporting Information), compared to that of the pristine graphene synthesized by a normal CVD method using CH_4 as the precursor. The appearance of D and D′ bands and an obvious blue shift (from 1585 to 1589 cm^{-1}) of the G band in N-doped graphene confirm the doping effect of N atoms. X-ray photoelectron spectroscopy (XPS) investigation (Figure S3 in Supporting Information) further verifies that N-doping or inclusion has been achieved in the graphene. Further, the amount of N-doping is correlated with the concentration of dopant element in the PAH precursor under the same growth conditions. For example, XPS data show that the atomic percentage of N-dopant in the HAT-CN and NPB samples is 7.8 and 3.1%, respectively, which is consistent with the higher N atomic concentration in HAT-CN compared to that in the NPB molecule. The carrier mobility of N-doped graphene from HAT-CN was measured at 1835 $cm^2\ V^{-1}\ s^{-1}$ without further optimization. Table 1 compares the present method quantitatively with other techniques that have been reported for growing graphene directly onto a substrate. The N- and F-co-doped graphene can also be obtained on the SiO_2/Si substrate at 1000 °C using hexadecafluorophthalocyanine copper(II) (F_{16}CuPc) as the solid carbon source (to be published elsewhere), which further confirms that the doping approach can be achieved if the suitable precursor is selected and the growth conditions are optimized.

Due to its excellent optical transparency and electrical conductivity, graphene is considered to be an ideal material to replace indium tin oxide (ITO) as a transparent electrode.[40−42] However, the complex transfer process of graphene onto transparent substrate usually introduces a variety of defects into the graphene sheet. The present method should provide a possible route to directly grow graphene on an arbitrary substrate, for example, quartz or glass, without the need for any transfer process. Table S1 in Supporting Information summarizes the parameters such as the layer number, transmittance, and square resistance of graphene prepared by different PAHs. Compared

TABLE 1. Comparison of Measured Parameters of Graphene Prepared through Different Methods

substrates	size (mm)	I_D/I_G	transmittance (%)	square resistance (KΩ/sq)	carrier mobility ($cm^2 V^{-1} s^{-1}$)	ref
SiO_2	limit by substrate	<0.2	N/A	N/A	~4400	18
quartz	~200	~0.2	82.0	0.27	~1500	26
Quartz	10	~1	84.0	30	N/A	27
$SrTiO_3$	limit by substrate	~1	96.4	0.95	870–1050	29
quartz	N/A	~2	~70	0.6	~200	28
glass or quartz	limit by substrate	<0.2	91.2	0.55	~1800	present work

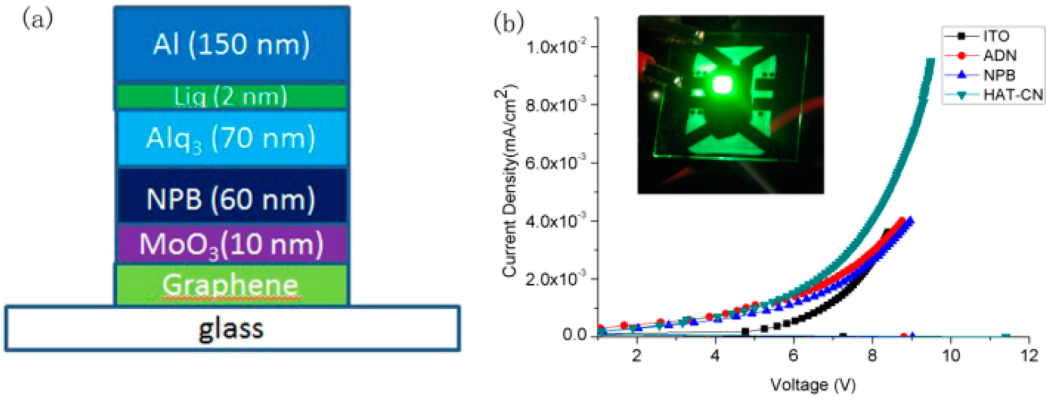

Figure 6. (a) Schematic of an OLED. (b) Characteristics of current density *vs* voltage for graphene devices and ITO devices. Inset is an image of the lit OLED with a graphene electrode.

with other PAHs, HAT-CN shows the lowest square resistance (550 Ω/sq) at 800 °C, and the square resistance is 850 Ω/sq at the lowest growth temperature (~600 °C) compatible with direct growth onto glass substrates. Due to the practical significance, we attempted to directly grow graphene on glass as a transparent electrode for organic light-emitting diode (OLED) application. After graphene growth, an OLED with the structure of glass/graphene/MoO_3/NPB/Alq_3/Liq/Al was directly fabricated (Figure 6a) on the graphene/glass. The performances of OLEDs fabricated on the graphene electrodes from different PAHs and on a reference ITO glass are compared in Figure 6b. Remarkably, the OLED fabricated on N-doped graphene from HAT-CN as the transparent electrode exhibits a higher current density than the ITO-based device operated at the same voltage (2.6 mA/cm^2 for ITO and 4.0 mA/cm^2 for N-doped graphene at 8 V). The picture of a lit OLED using graphene/glass electrode is shown in the inset. The luminance as a function of voltage for graphene and ITO OLEDs is also shown in Figure S4 (Supporting Information). Although as-synthesized graphene on glass can be used as the transparent electrode in OLEDs and shows higher current density than that of ITO, the other performances of the devices, such as turn on voltage, power luminance efficiency, *etc.*, cannot compete with ITO at the current stage without further engineering optimization of OLEDs on the graphene electrode. We believe that the method developed paves the way for transparent electrode applications of graphene.

CONCLUSIONS

In summary, we have developed a facile method for large-scale synthesis of doped and patterned graphene on an arbitrary substrate. High-quality graphene is obtained using a thin Cu layer as the top catalyst and PAHs as both carbon and doping sources at temperatures as low as 600 °C. The thicknesses of the Cu layer and PAHs are critical factors controlling the quality of graphene. The method has been demonstrated to successfully fabricate the graphene transparent electrode suitable for use in OLEDs. The present growth strategy provides a controllable transfer-free route for doped and patterned graphene growth, which will facilitate the practical applications of graphene.

METHODS

Synthesis of Graphene Film. First, 300 nm thick SiO_2/Si substrates were treated by Piranha solution (3:1 sulfuric acid/hydrogen peroxide). Then, PAHs and the Cu layer were deposited on it by thermal and e-beam evaporation (Kurt J. Lesker, PVD750), respectively. For the patterning, a shadow mask was applied during the PAHs and Cu layer deposition. After annealing in a Black Magic 4 in. R&D PECVD system (AIXTRON), graphene was synthesized between the Cu layer and the insulating substrate. Finally, the Cu layer was etched away by Marble's reagent ($CuSO_4$/HCl/H_2O = 10 g/50 mL/50 mL), and graphene was obtained directly on the SiO_2 substrate without

any transfer process. The process can be duplicated on other dielectric substrates such as glass or quartz to directly grow the graphene on the substrates.

Fabrication of OLEDs. The organic and metal layers were deposited on graphene/glass under a base pressure of 2×10^{-6} Torr by thermal evaporation through a shadow mask. The deposition rates were controlled and measured *in situ* using calibrated thickness monitors. After the deposition of all layers, four identical OLEDs with an emission area of 0.09 cm^2 were formed on the substrate. The EL characteristics of all the devices were evaluated using a Keithley 2400 sourcemeter constant current source and a PHOTO RESEARCH SpectraScan PR 655 photometer at room temperature.

Characterizations. Raman spectra and mapping images of graphene films were obtained on a Jobin-Yvon HR800 Raman spectrometer with a 633 nm wavelength incident laser at room temperature. The surface state and electron structure of the samples were obtained by XPS measurements (Kratos AXIS UltraDLD ultrahigh vacuum surface analysis system), using Al Kα radiation (1486 eV) as a probe. The thickness of graphene was measured by AFM (Veeco MultiMode V) under tapping mode. The scanning rate was 0.998 Hz, and the resonance vibration frequency was 350 kHz. *In situ* X-ray absorption fine structure spectra with a Cu *K*-edge were collected on Beamline BL14W1 at the Shanghai Synchrotron Radiation Facility (SSRF). XAFS data were acquired in the fluorescence mode through a self-designed *in situ* CVD cell in which the Cu/HAT-CN sample and reference Cu foil were annealed to 1000 °C during the XAFS measurement.

Conflict of Interest: The authors declare no competing financial interest.

Acknowledgment. The authors thank Beamline BL14W1 (Shanghai Synchrotron Radiation Facility) for providing the beam time. The authors thank Xiaochen Jiang and Jingyu Zhang for some carbon source evaporation, and Jiansheng Jie for providing different pattern masks. The work was supported by the Natural Science Foundation of China (NSFC) (Grant Nos. 91333112 and U1432249), the Priority Academic Program Development of Jiangsu Higher Education Institutions. This is also a project supported by Jiangsu Key Laboratory for Carbon-Based Functional Materials and Devices and Collaborative Innovation Center of Suzhou Nano Science & Technology, and sponsored by Qing Lan Project.

Supporting Information Available: Raman mapping spectra of I_G/I_D and I_{2D}/I_G patterned graphene (Figure S1) and Raman spectra of N-doped graphene synthesized by HAT-CN (Figure S2), XPS spectra of graphene grown with different PAHs (Figure S3), luminance as a function of voltage for graphene and ITO devices (Figure S4), and comparison of measured parameters of graphene prepared through different carbon sources (Table S1). This material is available free of charge *via* the Internet at http://pubs.acs.org.

REFERENCES AND NOTES

1. Huang, X.; Qi, X.; Boey, F.; Zhang, H. Graphene-Based Composites. *Chem. Soc. Rev.* **2012**, *41*, 666–686.
2. Guo, S.; Dong, S. Graphene Nanosheet: Synthesis, Molecular Engineering, Thin Film, Hybrids, and Energy and Analytical Applications. *Chem. Soc. Rev.* **2011**, *40*, 2644–2672.
3. Novoselov, K. S.; Geim, A. K.; Morozov, S. V.; Jiang, D.; Zhang, Y.; Dubonos, S. V.; Grigorieva, I. V.; Firsov, A. A. Electric Field Effect in Atomically Thin Carbon Films. *Science* **2004**, *306*, 666–669.
4. Novoselov, K. S.; Jiang, D.; Schedin, F.; Booth, T. J.; Khotkevich, V. V.; Morozov, S. V.; Geim, A. K. Two-Dimensional Atomic Crystals. *Proc. Natl. Acad. Sci. U.S.A.* **2005**, *102*, 10451–10453.
5. Su, C. Y.; Lu, A. Y.; Wu, C. Y.; Li, Y. T.; Liu, K. K.; Zhang, W.; Lin, S. Y.; Juang, Z. Y.; Zhong, Y. L.; Chen, F. R.; et al. Direct Formation of Wafer Scale Graphene Thin Layers on Insulating Substrates by Chemical Vapor Deposition. *Nano Lett.* **2011**, *11*, 3612–3616.
6. Li, X.; Magnuson, C. W.; Venugopal, A.; Tromp, R. M.; Hannon, J. B.; Vogel, E. M.; Colombo, L.; Ruoff, R. S. Large-Area Graphene Single Crystals Grown by Low-Pressure Chemical Vapor Deposition of Methane on Copper. *J. Am. Chem. Soc.* **2011**, *133*, 2816–2819.
7. Zhang, B.; Lee, W. H.; Piner, R.; Kholmanov, I.; Wu, Y. P.; Li, H. F.; Ji, H. X.; Ruoff, R. S. Low-Temperature Chemical Vapor Deposition Growth of Graphene from Toluene on Electropolished Copper Foils. *ACS Nano* **2012**, *6*, 2471–2476.
8. Zhuo, Q. Q.; Gao, J.; Peng, M. F.; Bai, L. L.; Deng, J. J.; Xia, Y. J.; Ma, Y. Y.; Zhong, J.; Sun, X. H. Large-Scale Synthesis of Graphene by the Reduction of Graphene Oxide at Room Temperature Using Metal Nanoparticles as Catalyst. *Carbon* **2013**, *52*, 559–564.
9. Gao, W.; Alemany, L. B.; Ci, L.; Ajayan, P. M. New Insights into the Structure and Reduction of Graphite Oxide. *Nat. Chem.* **2009**, *1*, 403–408.
10. Zhuo, Q.; Ma, Y.; Gao, J.; Zhang, P.; Xia, Y.; Tian, Y.; Sun, X.; Zhong, J.; Sun, X. Facile Synthesis of Graphene/Metal Nanoparticle Composites *via* Self-Catalysis Reduction at Room Temperature. *Inorg. Chem.* **2013**, *52*, 3141–3147.
11. Chen, F.; Tao, N. J. Electron Transport in Single Molecules: From Benzene to Graphene (vol 42, pg 429, 2009). *Acc. Chem. Res.* **2009**, *42*, 429–438.
12. Ravani, F.; Papagelis, K.; Dracopoulos, V.; Parthenios, J.; Dassios, K. G.; Siokou, A.; Galiotis, C. Graphene Production by Dissociation of Camphor Molecules on Nickel Substrate. *Thin Solid Films* **2013**, *527*, 31–37.
13. Ismach, A.; Druzgalski, C.; Penwell, S.; Schwartzberg, A.; Zheng, M.; Javey, A.; Bokor, J.; Zhang, Y. Direct Chemical Vapor Deposition of Graphene on Dielectric Surfaces. *Nano Lett.* **2010**, *10*, 1542–1549.
14. Byun, S.-J.; Lim, H.; Shin, G.-Y.; Han, T.-H.; Oh, S. H.; Ahn, J.-H.; Choi, H. C.; Lee, T.-W. Graphenes Converted from Polymers. *J. Phys. Chem. Lett.* **2011**, *2*, 493–497.
15. Pang, S.; Hernandez, Y.; Feng, X.; Mullen, K. Graphene as Transparent Electrode Material for Organic Electronics. *Adv. Mater.* **2011**, *23*, 2779–2795.
16. Chen, J. Y.; Wen, Y. G.; Guo, Y. L.; Wu, B.; Huang, L. P.; Xue, Y. Z.; Geng, D. C.; Wang, D.; Yu, G.; Liu, Y. Q. Oxygen-Aided Synthesis of Polycrystalline Graphene on Silicon Dioxide Substrates. *J. Am. Chem. Soc.* **2011**, *133*, 17548–17551.
17. Medina, H.; Lin, Y.-C.; Jin, C.; Lu, C.-C.; Yeh, C.-H.; Huang, K.-P.; Suenaga, K.; Robertson, J.; Chiu, P.-W. Metal-Free Growth of Nanographene on Silicon Oxides for Transparent Conducting Applications. *Adv. Funct. Mater.* **2012**, *22*, 2123–2128.
18. Shin, H. J.; Choi, W. M.; Yoon, S. M.; Han, G. H.; Woo, Y. S.; Kim, E. S.; Chae, S. J.; Li, X. S.; Benayad, A.; Loc, D. D.; et al. Transfer-Free Growth of Few-Layer Graphene by Self-Assembled Monolayers. *Adv. Mater.* **2011**, *23*, 4392–4397.
19. Kwak, J.; Chu, J. H.; Choi, J. K.; Park, S. D.; Go, H.; Kim, S. Y.; Park, K.; Kim, S. D.; Kim, Y. W.; Yoon, E.; et al. Near Room-Temperature Synthesis of Transfer-Free Graphene Films. *Nat. Commun.* **2012**, *3*, 645.
20. Medina, H.; Lin, Y. C.; Jin, C. H.; Lu, C. C.; Yeh, C. H.; Huang, K. P.; Suenaga, K.; Robertson, J.; Chiu, P. W. Metal-Free Growth of Nanographene on Silicon Oxides for Transparent Conducting Applications. *Adv. Funct. Mater.* **2012**, *22*, 2123–2128.
21. Hwang, J.; Kim, M.; Campbell, D.; Alsalman, H. A.; Kwak, J. Y.; Shivaraman, S.; Woll, A. R.; Singh, A. K.; Hennig, R. G.; Gorantla, S.; et al. van der Waals Epitaxial Growth of Graphene on Sapphire by Chemical Vapor Deposition without a Metal Catalyst. *ACS Nano* **2013**, *7*, 385–395.
22. Song, H. J.; Son, M.; Park, C.; Lim, H.; Levendorf, M. P.; Tsen, A. W.; Park, J.; Choi, H. C. Large Scale Metal-Free Synthesis of Graphene on Sapphire and Transfer-Free Device Fabrication. *Nanoscale* **2012**, *4*, 3050–3054.
23. Ding, X.; Ding, G.; Xie, X.; Huang, F.; Jiang, M. Direct Growth of Few Layer Graphene on Hexagonal Boron Nitride by Chemical Vapor Deposition. *Carbon* **2011**, *49*, 2522–2525.
24. Lin, T.; Liu, Z.; Zhou, M.; Bi, H.; Zhang, K.; Huang, F.; Wan, D.; Zhong, Y. Rapid Microwave Synthesis of Graphene Directly on h-BN with Excellent Heat Dissipation Performance. *ACS Appl. Mater. Interfaces* **2014**, *6*, 3088–3092.

25. Chen, J.; Guo, Y.; Jiang, L.; Xu, Z.; Huang, L.; Xue, Y.; Geng, D.; Wu, B.; Hu, W.; Yu, G.; et al. Near-Equilibrium Chemical Vapor Deposition of High-Quality Single-Crystal Graphene Directly on Various Dielectric Substrates. *Adv. Mater.* **2014**, *26*, 1348–1353.
26. Xu, S.; Man, B.; Jiang, S.; Yue, W.; Yang, C.; Liu, M.; Chen, C.; Zhang, C. Direct Growth of Graphene on Quartz Substrates for Label-Free Detection of Adenosine Triphosphate. *Nanotechnology* **2014**, *25*, 165702.
27. Zhang, Z.; Guo, Y.; Wang, X.; Li, D.; Wang, F.; Xie, S. Direct Growth of Nanocrystalline Graphene/Graphite Transparent Electrodes on Si/SiO_2 for Metal-Free Schottky Junction Photodetectors. *Adv. Funct. Mater.* **2014**, *24*, 835–840.
28. Yen, W.-C.; Chen, Y.-Z.; Yeh, C.-H.; He, J.-H.; Chiu, P.-W.; Chueh, Y.-L. Direct Growth of Self-Crystallized Graphene and Graphite Nanoballs with Ni Vapor-Assisted Growth: From Controllable Growth to Material Characterization. *Sci. Rep.* **2014**, *4*, 4739.
29. Sun, J.; Gao, T.; Song, X.; Zhao, Y.; Lin, Y.; Wang, H.; Ma, D.; Chen, Y.; Xiang, W.; Wang, J.; et al. Direct Growth of High-Quality Graphene on High-kappa Dielectric $SrTiO_3$ Substrates. *J. Am. Chem. Soc.* **2014**, *136*, 6574–6577.
30. Chen, J. Y.; Guo, Y. L.; Jiang, L. L.; Xu, Z. P.; Huang, L. P.; Xue, Y. Z.; Geng, D. C.; Wu, B.; Hu, W. P.; Yu, G.; et al. Near-Equilibrium Chemical Vapor Deposition of High-Quality Single-Crystal Graphene Directly on Various Dielectric Substrates. *Adv. Mater.* **2014**, *26*, 1348–1353.
31. Yan, Z.; Peng, Z. W.; Sun, Z. Z.; Yao, J.; Zhu, Y.; Liu, Z.; Ajayan, P. M.; Tour, J. M. Growth of Bilayer Graphene on Insulating Substrates. *ACS Nano* **2011**, *5*, 8187–8192.
32. Xue, Y.; Wu, B.; Jiang, L.; Guo, Y.; Huang, L.; Chen, J.; Tan, J.; Geng, D.; Luo, B.; Hu, W.; et al. Low Temperature Growth of Highly Nitrogen-Doped Single Crystal Graphene Arrays by Chemical Vapor Deposition. *J. Am. Chem. Soc.* **2012**, *134*, 11060–11063.
33. Gebhardt, J.; Koch, R. J.; Zhao, W.; Hofert, O.; Gotterbarm, K.; Mammadov, S.; Papp, C.; Gorling, A.; Steinruck, H. P.; Seyller, T. Growth and Electronic Structure of Boron-Doped Graphene. *Phys. Rev. B* **2013**, *87*, 155437.
34. Zhang, C.; Fu, L.; Liu, N.; Liu, M.; Wang, Y.; Liu, Z. Synthesis of Nitrogen-Doped Graphene Using Embedded Carbon and Nitrogen Sources. *Adv. Mater.* **2011**, *23*, 1020–1024.
35. Wan, X.; Chen, K.; Liu, D.; Chen, J.; Miao, Q.; Xu, J. High-Quality Large-Area Graphene from Dehydrogenated Polycyclic Aromatic Hydrocarbons. *Chem. Mater.* **2012**, *24*, 3906–3915.
36. Ji, H.; Hao, Y.; Ren, Y.; Charlton, M.; Lee, W. H.; Wu, Q.; Li, H.; Zhu, Y.; Wu, Y.; Piner, R.; et al. Graphene Growth Using a Solid Carbon Feedstock and Hydrogen. *ACS Nano* **2011**, *5*, 7656–7661.
37. Sun, Z.; Yan, Z.; Yao, J.; Beitler, E.; Zhu, Y.; Tour, J. M. Growth of Graphene from Solid Carbon Sources. *Nature* **2010**, *468*, 549–552.
38. Ago, H.; Ogawa, Y.; Tsuji, M.; Mizuno, S.; Hibino, H. Catalytic Growth of Graphene: Toward Large-Area Single-Crystalline Graphene. *J. Phys. Chem. Lett.* **2012**, *3*, 2228–2236.
39. Park, H. J.; Meyer, J.; Roth, S.; Skákalová, V. Growth and Properties of Few-Layer Graphene Prepared by Chemical Vapor Deposition. *Carbon* **2010**, *48*, 1088–1094.
40. Kim, K. S.; Zhao, Y.; Jang, H.; Lee, S. Y.; Kim, J. M.; Ahn, J. H.; Kim, P.; Choi, J. Y.; Hong, B. H. Large-Scale Pattern Growth of Graphene Films for Stretchable Transparent Electrodes. *Nature* **2009**, *457*, 706–710.
41. Han, T. H.; Lee, Y. B.; Choi, M. R.; Woo, S. H.; Bae, S. H.; Hong, B. H.; Ahn, J. H.; Lee, T. W. Extremely Efficient Flexible Organic Light-Emitting Diodes with Modified Graphene Anode. *Nat. Photonics* **2012**, *6*, 105–110.
42. Kim, H.; Bae, S. H.; Han, T. H.; Lim, K. G.; Ahn, J. H.; Lee, T. W. Organic Solar Cells Using CVD-Grown Graphene Electrodes. *Nanotechnology* **2014**, *25*, 014012.